ECOLE POLYTECHNIQUE

CENTRE DE MATHÉMATIQUES APPLIQUÉES

UMR CNRS 7641

91128 PALAISEAU CEDEX (FRANCE). Tél: 01 69 33 46 00. Fax: 01 69 33 46 46
http://www.cmap.polytechnique.fr/

On the activation of a fasciculus of axons

Emmanuela Mandonnet, Olivier Pantz

R.I. 714 *Juin 2011*

On the activation of a fasciculus of axons

E. Mandonnet[a], O. Pantz[b]

[a] *Lariboisière Hospital, Paris, France*
[b] *CMAP, Ecole Polytechnique, Route de Saclay, 91128 Palaiseau Cedex*

Abstract

Direct electrical stimulation of cortical and axonal areas is widely used for brain mapping of functional areas during intraparenchymatous resections. Direct access to the precise area activated by a given stimulation, is difficult to observe experimentally. The aim of this article is to present a numerical method to compute this area. As axonal fasciculus are made of a large number of axons, direct computations on the genuine geometry are out of reach. In consequence, we use a homogenization process allowing us to approximate the full microscopic heterogeneous system by a homogeneous macroscopic one. The obtained modeling is known as the bidomain model and has been previously used for the study of syncytial tissues. Numerical simulations are performed using a finite element method.

Keywords: neurone, activating function

1. Introduction

Ojemann's stimulation is considered to be the gold standard for brain function mapping during awake surgery. It consists to apply an electrical stimulation using a bipolar electrode to a fasciculus of axons. As soon as the jump of the electric potential across the membranes of an axon exceeds a given threshold, it is activated: a signal that propagates along the axons is generated. This technique enables the surgeon to determine the functional role of the stimulated bundle of axons and thus to avoid resections of crucial area. In this context it is essential to determine what is the precise area activated by the stimulation. As in vivo measures appears to be difficult to carry out, we propose to compute this area numerically.

A fasciculus of axons is a collection of axons embedded into an external matrix. The electric potential satisfies a Poisson equation inside and outside the axons. What is more, the interface between the two domains is made of a membrane that has its own resistivity and capacitance. Solving the whole system numerically is completely out of reach in practice. In order to overcome this problem, it is natural to seek for a macroscopic homogeneous equivalent to the heterogeneous microscopic one (a process known as homogenization). Moreover, such an approach has an interest for itself as it throws a new light on the physical phenomena at stake. The homogenization process leads to a bidomain modeling. In this framework, the state of the system is described at each point of the domain by both external and internal potentials that satisfy a coupled system of diffusion equations. Such a modeling has already been formally derived in the context of syncytial tissues by Krassowska and Neu [11] (see also [1, 8, 9]). A rigorous justification of the homogenized limit has been proposed by Pennacchio and Al [12], based on a variational approach, following the work of De Giorgi [3, 5, 4]. The mathematical theory of homogenization dates back to the seventies and a first approach was proposed by Spagnolo [13, 14], Tartar and Murat [15, 10] and had since been applied to a large body of different systems. We refer the reader to recent monographs for a historical background and the references therein [2, 6, 7]. Even though the equations at the microscopic scales are identical for syncytial tissues and fasciculus of axons, it seems that the homogeneous method as never been applied to the latter case. The only main difference lies in the geometry of the fibers that are disconnected from one another when axons are considered contrarily to syncytial tissues. This leads to a degenerate conductivity for the internal potential. It seems that the approach used by Pennachio and Al in [12] could be extended to this case with minor changes. Finally, let us underline that we only consider the case of passive

Email address: olivier.pantz@polytecnique.org (O. Pantz)
URL: http://www.cmap.polytechique.fr (O. Pantz)

interface between the two media. Thus is our modeling only a rough approximation of the reality and can be considered as valid as long as the activation threshold is not reached. In particular it could not enable us to simulate the propagation of a signal along the axons. The possibility to extend similar analysis to a non linear response of the membrane such as the one introduced by Hodgkin-Huxley should be investigated in the future.

The first part of this article is devoted to the setting of the problem. We first present the full three-dimensional modeling on the genuine geometry 2.1. The homogenized model is introduced in 2.2 where expression of the homogenized coefficients in function of the parameters and geometry at the microscopic level are also given. We show in section 2.3 that the standard modeling commonly used for axonal activation can be obtained as an approximation of the bidomain model in the case of a low density of axons. This part ends with 2.4 on a brief discussion on the activating function, a popular tool among biologists to compute the activated area.
Section 3 is devoted to the presentation of the numerical simulations. The numerical scheme, based on the finite element method is presented in 3.1, whereas section 3.2 is devoted to the results obtained. In particular, we compare the dependence of the response on the applied intensity and on the orientation of the bipolar electrode with respect to the orientation of the fibers. Moreover, we compare the results obtained using the homogenized bidomain model to the output given by the simpler – and widely used – low axonal density approximation.

2. Modeling

2.1. Full three dimensional modeling

We consider a bundle of axons, assumed to be of infinite length embedded in a cylindric domain

$$\Omega = \omega \times \mathbb{R},$$

where ω is an open subset of $\mathbb{R}^2$. The axons are assumed to be oriented along e_3, where (e_1, e_2, e_3) is the canonical basis of $\mathbb{R}^3$. The domain Ω is the union of an external matrix $\Omega_e = \omega_e \times \mathbb{R}$ and of the domain occupied by the axons denoted $\Omega_i = \omega_i \times \mathbb{R}$ with $\overline{\omega_i} \subset \omega$, where ω_i and ω_e are the domains occupied respectively by the axons and the external matrix in a section ω of the domain. The electric potential u satisfies the Poisson equation in the matrix and in the axons, that is

$$-\nabla \cdot M_e \nabla u = 0 \text{ in } \Omega_e \text{ and } -\nabla \cdot M_i \nabla u = 0 \text{ in } \Omega_i,$$

where M_e and M_i are the conductivities of the medium of the matrix and of the axons respectively. The interface $\Gamma = \partial\Omega_e \cap \partial\Omega_i$ between the external matrix and the axons is constituted by a membrane which partially isolates the inner domain occupied by the axons with the external matrix, thus allowing jump of the potential across it. At rest, the jump of the potential is not zero but is equal to a given value δV. The current across the membrane depends on the jump of the potential (resistivity effect) and on the time derivative of its jump (capacity effect). More precisely, we have

$$M_e \nabla u_e \cdot n = M_i \nabla u_i \cdot n = C \frac{\partial [u]}{\partial t} + R([u] - \delta V) \text{ on } \Gamma,$$

where u_e and u_i denote the respectively the potential in the matrix and in the axons, C is the capacitance of the membrane, R is its conductance and

$$[u] = u_i - u_e$$

is the jump of the potential across the membrane. We assume the membrane to be passive, that is δV, R and C to be constant. A more realistic modeling should take into account the fact that the ionic channels of the membrane can close or open themselves according to both the value of the jump of the potential and the ionic concentrations. For such a modeling, the membrane conductivity R and the jump of the potential δV could not be assumed to be constant. This feature enables the propagation of a signal along the axons. The approximation made here is roughly valid till the axons are not activated. Limit conditions has to be supplemented on the boundary of Ω to close the system. On the part of the boundary Γ_N where the electrodes are applied, we have

$$M_e \nabla u_e \cdot n = g(t) \text{ on } \Gamma_N \tag{1}$$

where g is the current by surface unit applied at the electrodes and n the outward normal to the domain. On the remaining of the boundary, we assume the flux to be zero.

$$M_e \nabla u_e \cdot n = 0 \text{ in } \partial\Omega \setminus \Gamma_N. \tag{2}$$

Moreover, the external potential u_e is assumed to go to zero at infinity

$$\lim_{|x| \to +\infty} u_e(x) = 0,$$

and the inner flux to be zero at infinity

$$\lim_{|x| \to +\infty} M_i \partial_3 u_i(x) = 0.$$

Finally, initial conditions on the jump of u as to be added

$$[u](t = 0) = [u_0],$$

where $[u_0]$ is the initial jump of the potential at time $t = 0$ (usually, $[u_0]$ will be taken equal to δV).

2.2. Homogenization

Because of the important number of axons per unit section, a direct numerical resolution of the previous system is almost out of reach. In order to overcome this problem, we propose to homogenize the system, that is to replace the full heterogeneous system by a homogeneous one. From the mathematical viewpoint it consists to perform an asymptotic analysis by letting the concentration of the axons go to infinity while letting their diameter go to zero and to identify the limit modeling. Such an analysis leads to a coupled system set on Ω where the unknowns are the external and internal potentials u_e and u_i. The homogenized system reads as follow

$$-\nabla \cdot (M_e^* \nabla u_e) - C^* \frac{\partial [u]}{\partial t} - R^*([u] - \delta V) = 0 \text{ in } \Omega, \quad (3)$$

$$-\partial_3 (M_i^* \partial_3 u_i) + C^* \frac{\partial [u]}{\partial t} + R^*([u] - \delta V) = 0 \text{ in } \Omega \quad (4)$$

with $[u] = u_i - u_e$ and

$$M_e^* \nabla u_e \cdot n = g \text{ in } \Gamma_N$$

while

$$M_e^* \nabla u_e \cdot n = 0 \text{ in } \partial\Omega \setminus \Gamma_N,$$

together with the conditions at infinity

$$\lim_{|x| \to +\infty} u_e(x) = 0, \qquad \lim_{|x| \to +\infty} M_i^* \partial_3 u_i(x) = 0.$$

The constants M_e^*, M_i^* are the homogenized conductivities of the medium of the matrix and of the axons respectively, R^* is the homogenized conductivity of the membranes of the axons and C^* is their homogenized capacity. The values of those homogenized constants depend on their non-homogenized counterparts and on the density and diameter of the axons. We have

$$M_i^* = \rho M_i^0, \quad M_i^0 = \frac{\pi d^2}{4} \inf_{\zeta \in \mathbb{R}^2} M_i(\zeta + e_3) \cdot (\zeta + e_3),$$

$$C^* = \rho C_i^0, \quad C_i^0 = d\pi C,$$

and

$$R^* = \rho R_i^0, \quad R_i^0 = d\pi R.$$

Moreover the external homogenized conductivity M_e^* also depends on the geometric arrangement of the axons at the microscopic level. Even if the initial conductivities are isotropic, it is not necessarily the case for M_e^*. It is possible to compute an approximation of the homogenized external conductivity if the axons are organized along a periodic lattice. For instance, if we assume them to be organized along a square lattice, we get

$$M_e^* \xi \cdot \xi = \inf_{v \in H^1_\#(Y_e)} |Y|^{-1} \int_{Y_e} M_e \left(\xi + \nabla_y v\right) \cdot \left(\xi + \nabla_y v\right) dy, \quad (5)$$

where $Y =]0,1[^2$ is the periodicity cell, $Y_e \subset Y$ is the subset of Y occupied by the external matrix and $H^1_\#(Y_e)$ is the Y-periodic functions on Y_e that admits an L^2 weak derivative (the infimum could also simply be taken over the set of Y-periodic regular functions on Y_e without any change on the result).

2.3. Case of low axon density

The equations satisfied by u_e and u_i can be rewritten in terms of u_e and $[u]$. Moreover, using the definition of M_i^*, R^* and C^* we deduce from (3-4), that

$$-\nabla \cdot (M_e^* \nabla u_e) = \rho \left(C^0 \frac{\partial [u]}{\partial t} - R^0([u] - \delta V) \right), \quad (6)$$

$$-\partial_3 (M_i^0 \partial_3 [u]) + C^0 \frac{\partial [u]}{\partial t} + R^0([u] - \delta V) = -\partial_3 (M_i^0 \partial_3 u_e). \quad (7)$$

Most models proposed in the literature do assume the external potential u_e to be independent of u_i. Such a hypothesis is valid for a low density of axons. Indeed, as M_e^* converges to M_e as ρ goes to zero, (6) leads to

$$-\nabla \cdot (M_e \nabla u_e) = 0 \text{ in } \Omega. \quad (8)$$

In such a case, the initial system is no more coupled, as u_e can be computed independently of $[u]$ and only depends on the applied current g.

2.4. Activating Function

The activating function is defined as the source term of equation (7), that is

$$f = -\partial_3 (M_i^0 \partial_3 u_e).$$

Let us assume that $[u] = \delta V$ at time $t = 0$. If no stimulation is applied (that is $u_e = 0$), we have $f = 0$ and $[u] = \delta V$ for all time $t > 0$. Moreover, if we assume $[u]$ to be regular, we get

$$[u](t) = \delta V + (C^0 f)t + o(t),$$

with $o(t)/t$ converging toward zero when t goes to zero. Assuming that the activation of the axons is triggered when $[u]$ reaches a given potential of activation δU, and using the latter approximation of $[u]$, the activated axons are the one for which

$$(\delta U - \delta V)^{-1} C^0 t \geq f. \quad (9)$$

It follows that the greater f is the more quicker an axon is activated.
Nevertheless, the use of the activating function to determine the activated area is quite questionable. First it relies on several assumptions that are not necessarily verified: low density of axons and regularity of $[u]$ with respect to the time (which is not expected near the electrodes). Moreover, criteria (9) can only be used for small time t (extending it to any time t will lead to an overestimation of the activated area). An estimation of the activated area only based on the activating function f requires the introduction of an arbitrary threshold $f_a > 0$, so to be defined as the elements $x \in \Omega$ such that

$$f(x) \geq f_a.$$

The result will obviously strongly relies on the choice f_a made. The introduction of such a threshold is not required if the whole coupled system (3-4) is solved, what we proposed to do in the next section. If the axons density is low, system (7-8) can be used as well.

3. Numerical Simulations

In order to solve (3-4) we use a finite elements discretization in space and a finite difference discretization in time.

3.1. Numerical Scheme

Spatial discretization. Multiplying equation (3) by a test function v_e and integrating over Ω, we obtain, using (1-2), after an integration by part that

$$\int_\Omega M_e^* \nabla u_e \cdot \nabla v_e \, dx + \int_\Omega C^* \frac{\partial [u]}{\partial t} v_e - R^*([u] - \delta V) v_e \, dx = \int_\Gamma g v_e \, ds.$$

Multiplying (4) by a test function v_i and integrating over Ω leads to

$$\int_\Omega M_i^* \partial_3 u_i \partial_3 v_i \, dx - \int_\Omega C^* \frac{\partial [u]}{\partial t} v_i - R^*([u] - \delta V) v_i \, dx = 0.$$

By summation of those two equations, we get that for all test functions v_e and v_i,

$$\int_\Omega C^* \frac{\partial [u]}{\partial t} [v] + R^*([u] - \delta V)[v] + M_e^* \nabla u_e \cdot \nabla v_e + M_i^* \partial_3 u_i \partial_3 v_i \, dx = \int_\Gamma g v_e \, ds, \quad (10)$$

with

$$[u](t = 0) = \delta V. \quad (11)$$

In order to use a finite elements space discretization, we first begin to truncate the domain. Let L be a positive real, we set

$$\Omega_L = \omega \times]-L, L[.$$

We assume that L is large enough so that $\Gamma \subset \partial\Omega_L$ and we denote by $u^L = (u_e^L, u_i^L)$ the approximation of $u = (u_e, u_i)$ solution of the system

$$C^* \frac{d}{dt}([u^L], [v])_{L^2} + a(u^L, v) = L_t(v), \quad (12)$$

for all test functions $v = (v_e, v_i)$ such that $v_e = 0$ on $\omega \times \{-L, L\}$ with

$$u_e^L = 0 \text{ on } \omega \times \{-L, L\} \quad (13)$$

and

$$[u^L](t = 0) = \delta V, \quad (14)$$

where

$$([u], [v])_{L^2} = \int_{\Omega_L} [u][v] \, dx,$$

$$a(u, v) = \int_{\Omega_L} R^*[u][v] + M_e^* \nabla u_e \cdot \nabla v_e + M_i^* \partial_3 u_i \partial_3 v_i \, dx$$

and

$$L_t(v) = \int_\Gamma g(t) v_e \, ds + \int_\Omega R^* \delta V [v].$$

The finite element method consists in solving (12 - 14) on a finite dimensional space

$$X_h \subset \Big\{(v_e, v_i) : \Omega_L \to \mathbb{R} \times \mathbb{R} \text{ such that } v_e = 0 \text{ on } \omega \times \{-L, L\}\Big\}, \Big\},$$

that is to find

$$(u_e^L, u_i^L) \in C^0([0, T], L^2(\Omega)^2) \cap L^2(]0, T[, X_h),$$

such that (14) is satisfied together with (12) for all $(v_e, v_i) \in X_h$. Different finite element spaces could be used to define X_h. In the simulation presented thereafter, we have use P_1 Lagrange finite elements, that is

$$X_h = \Big\{(v_e, v_i) \in C^0(\Omega)^2 \text{ such that } v_e = 0 \text{ on } \Gamma_N \text{ and for all triangles } K \in \mathcal{T}_h \quad v_e|_K, v_i|_K \in \Pi_1\Big\},$$

where $\mathcal{T}_h$ is a conform tetrahedral mesh of the domain Ω_L and Π_1 is the set of affine functions from $\mathbb{R}^3$ into $\mathbb{R}$.

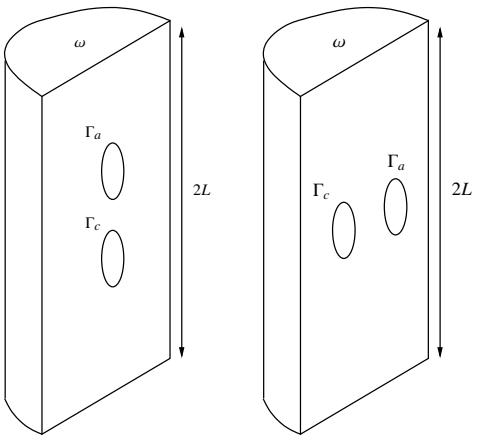

Figure 1: Domain Ω_L of computation

Time discretization. We denote by u_n^L the computed approximation of u^L at time $t_n = n\Delta t$, where Δt is a small time step. We use an implicit scheme to solve (12 - 14) on X_h, consisting to compute the sequence $u_n^L \in X_h$ such that for all $v \in X_h$ and all $n \geq 0$,

$$C^*\left(\frac{[u_{n+1}^L - u_n^L]}{\Delta t}, [v]\right)_{L^2} + a(u_{n+1}^L, v) = L_{t_{n+1}}(v), \quad (15)$$

with

$$[u_0^L] = \delta V. \quad (16)$$

At each time step $n \geq 0$, (15) is nothing more than a linear system. Other time discretization can be used. Moreover, it is also possible to adapt the time step Δt in order to speed up the computations.

3.2. Numerical Results

Geometry of the domain. We chose ω to be half a disk of radius r

$$\omega = \{(x, y) \in \mathbb{R} \times \mathbb{R}^- : \ x^2 + y^2 \leq r^2\}.$$

We recall that Ω_L is the cylinder of base ω of half height L, that is

$$\Omega_L = \omega \times]-L, L[.$$

The electrodes are assumed to be in contact with the domain Ω_L on $\Gamma = \Gamma_a \cup \Gamma_c$, where Γ_a and Γ_c are disks of radius r_c of respective center x_a and x_c included in the flat part $]-r, r[\times\{0\}\times]-L, L[$ of the boundary of Ω_L. The distance between the centers of Γ_a and Γ_c is denoted δ_c. We will consider two cases. The electrodes will be placed either parallel to the direction of the axons (see figure 1)

$$x_a = (0, 0, \delta_c/2) \text{ and } x_c = (0, 0, -\delta_c/2) \quad (\mathrm{H}_{\|})$$

or orthogonal to the direction of the axons

$$x_a = (\delta_c/2, 0, 0) \text{ and } x_c = (-\delta_c/2, 0, 0). \quad (\mathrm{H}_{\perp})$$

Applied pulse. A periodic biphasic pulse is applied at the electrodes. More precisely, we defined $g(t)$ on Γ_a by

$$g(t) = \begin{cases} I/|\Gamma_a| & \text{for all } t \in]0, T_p[\\ -I/|\Gamma_a| & \text{for all } t \in]T_p, 2T_p[\\ 0 & \text{for all } t \in]2T_p, T[\end{cases},$$

whereas on Γ_c,

$$g(t) = \begin{cases} -I/|\Gamma_a| & \text{for all } t \in]0, T_p[\\ I/|\Gamma_a| & \text{for all } t \in]T_p, 2T_p[\\ 0 & \text{for all } t \in]2T_p, T[\end{cases}$$

where T_p is the pulse time, T is the overall period of stimulation and I the intensity of the pulse.

Physical constants. The simulations have been performed using physical values given by table 1. The homogenized conductivity law M_e^* given by (5) of the external matrix has been computed using a finite element method and assuming the axons to be arranged on a squared periodic lattice. We obtain that (in S/m)

$$M_e^* = \begin{pmatrix} 0.174 & 4.510^{-7} & 0 \\ 4.510^{-7} & 0.174 & 0 \\ 0 & 0 & 0.228614 \end{pmatrix}.$$

The assumption that the axons are arranged along a squared periodic lattice introduces a small anisotropy of the transversal conductivity. Moreover, the conductivity of the external matrix is slightly greater along the direction of the axons than in transversal one. Note that the total conductivity, taking also the axons into account, is even more anisotropic as the longitudinal conductivity is the sum of the external and internal ones (that is about $0.35 S/m$ compared with $0.174 S/m$ for the transversal conductivity).

Meshing of the domain. The computation has been performed on a mesh containing approximatively 15000 tetrahedrons (exact value depends on the case considered). It has been refine around the electrodes, where the solution is the less regular.

Variable	Notation	value	units
Radius of the domain	r	15.e-3	m
Length of the domain	L	40.e-3	m
Distance between the center of the electrodes	δ_c	7.e-3	m
Radius of the contact	r_c	1.e-3	m
Pulse time	T_p	5.e-4	s
Stimulation period	T	0.02	s
Applied intensity	I	0.5 to 5	mA
Matrix conductivity	M_e	1/3	S/m
Axon conductivity	M_i	1	S/m
Membrane conductivity	R	0.15	S/m^2
Membrane capacitance	C	6.e-7	F/m
Axon diameter	d	2.e-6	m
Axon density	ρ	1.e11	m^{-2}

Table 1: Numerical values used for the simulations

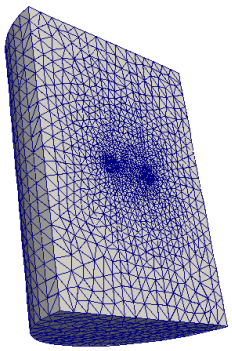

Figure 2: Meshing of the domain (orthogonal configuration)

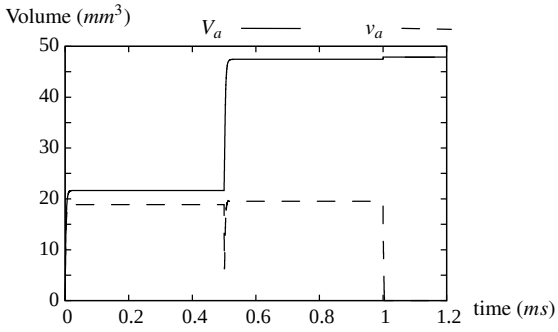

Figure 3: Activation Volume for the orthogonal configuration with $I = 5mA$

Activated Volume. We defined the activated area $\omega_a(t)$ at time t as the set of elements of the domain for which the jump of the potential exceeds the activation threshold δU

$$\omega_a(t) = \{x \text{ such that } [u](x,t) > \delta U\}.$$

We denote by $\Omega_a(t)$ the activated area during time interval $(0,t)$, that is

$$\Omega_a(t) = \bigcup_{s\in(0,t)} \omega_a(s)$$

and by

$$v_a(t) = |\omega_a(t)| \text{ and } V_a(t) = |\Omega_a(t)|$$

the volume of the activated areas at time t and during time interval $(0,t)$. The graphs of the activated volumes at time t and during time $(0,t)$ are displayed on Figure 3 where the intensity I has been chosen equal to $5mA$.

First, it shows that the activated volume is merely constant after each change of the applied pulse after a brief transition phase. At first sight, we could have conclude that the time dependent modeling could be replaced by a quasi-static one and neglect the transition phases. This would be unwise, as it would lead to an underestimation of the total activated area. Indeed, as v_a is not equal to V_a on $(0,T_p)$, the activated area $\omega_a(t)$ is not monotonously growing during the first phase $(0,T_p)$. A quasi-static modeling would lead to a total activated area equal to $v_a(T_p^-)$ instead of $V_a(T_p^-)$.

Activated areas. The activated areas during time $(0,T)$ are displayed on Figures (4) and (5) for the orthogonal and parallel configurations respectively and different applied intensities. Colors correspond to the maximum jump of potential reached during the cycle $[0,T]$. We

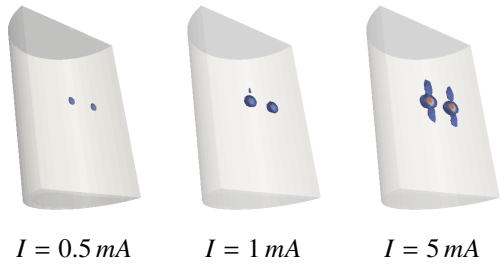

Figure 4: Activated area for different intensities (orhtogonal configuration)

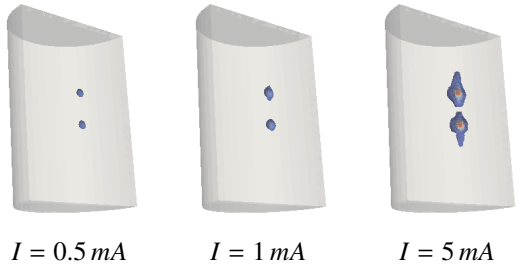

Figure 5: Activated area for different intensities (parallel configuration)

obtain that the activated area is mainly localized around the contact zone with the electrodes. Let us underline that the area in between the two electrods is not activated. The effect due to the anisotropy could only be observed for relatively high intensities. Figures (7) and (6) display a zoom of the activated areas in the orthogonal configuration.

Orthogonal versus Parallel configurations. It is usually common to believe that placing the electrodes parallel to the axons leads to the strongest response (that is a largest activated area for a given intensity). Figure 8, which compares the activated volume over a time interval $(0, t)$ for orthogonal and parallel configurations, suggests on the contrary that responses are quite comparable in both cases. In consequences, it doesn't seem that the parallel configuration should especially be favored.

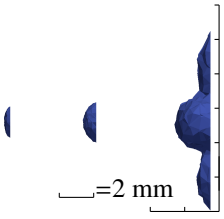

Figure 6: Activated Area for I =0.5, 1, 5 mA (from left to right)

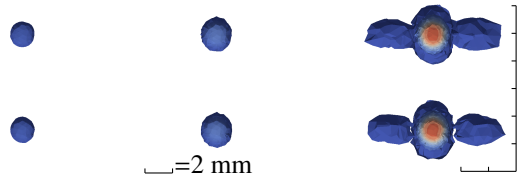

Figure 7: Activated Area for I =0.5, 1, 5 mA (from left to right)

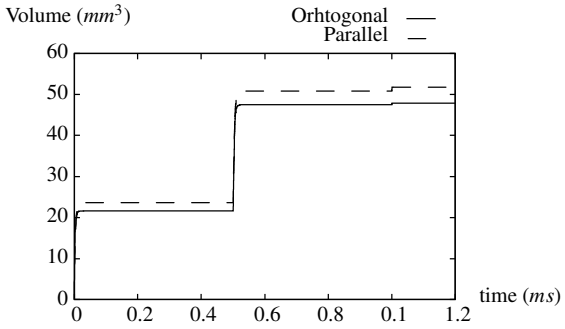

Figure 8: Activation volumes for the orthogonal and parallel settings, with I = 5 mA.

Low density modeling. As previously underlined, most articles found in the literature do focus on the study of a single axon placed in a given external potential field. This leads to equations (7-8), where the external field is considered to be independent of the jump of the potential. Being uncoupled, this system is much more easy to solve than the full one and it is natural to try to figure out to which extend it can be used. To this end, we compared the activated volume obtained for each modeling with the same set of data. Figure (9) displays the activated volume with an applied current of intensity $I = 5\,mA$. The results are qualitatively comparable, but the activated area is approximately underestimated by 20%.

4. Conclusion

The use of homogenization techniques in the context of the study of fasciculus of axons seems to open new perspectives. On one hand, the homogenized system is simple enough to be solved numerically. On the other, it provides an interesting viewpoint that enable us for instance to understand why the behavior of the system

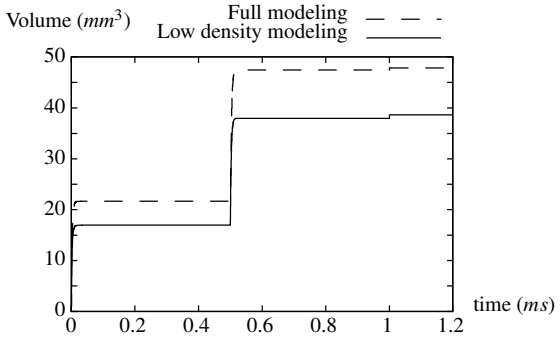

Figure 9: Activation Volumes for low density and full modelings with $I = 5mA$ in the orthogonal configuration.

is non isotropic even if both inner and external conductivities at a microscopic level are. The simulations we have performed suggest that the orientation the bipolar electrode with respect to the orientation of the fibers has no major influence on the activated area – contrarily to a widespread belief that they should be placed parallel to the axons. Moreover, the activation area is located right under the tips of the electrods, whereas the region in between them is not activated. Future works should extend our analysis to more realistic non-linear modeling of the membrane of the axons.

References

[1] P. Colli Franzone and G. Savaré. Degenerate evolution systems modeling the cardiac electric field at micro- and macroscopic level. In *Evolution equations, semigroups and functional analysis (Milano, 2000)*, volume 50 of *Progr. Nonlinear Differential Equations Appl.*, pages 49–78. Birkhäuser, Basel, 2002.

[2] G. Dal Maso. *An introduction to Γ-convergence*. Progress in Nonlinear Differential Equations and their Applications, 8. Birkhäuser Boston Inc., Boston, MA, 1993.

[3] E. De Giorgi. Sulla convergenza di alcune successioni d'integrali del tipo dell'area. *Rend. Mat. (6)*, 8:277–294, 1975. Collection of articles dedicated to Mauro Picone on the occasion of his ninetieth birthday.

[4] E. De Giorgi. *G*-operators and Γ-convergence. In *Proceedings of the International Congress of Mathematicians, Vol. 1, 2 (Warsaw, 1983)*, pages 1175–1191, Warsaw, 1984. PWN.

[5] E. De Giorgi and T. Franzoni. Su un tipo di convergenza variazionale. *Atti Accad. Naz. Lincei Rend. Cl. Sci. Fis. Mat. Natur. (8)*, 58(6):842–850, 1975.

[6] U. Hornung. Introduction. In *Homogenization and porous media*, volume 6 of *Interdiscip. Appl. Math.*, pages 1–25, 259–275. Springer, New York, 1997.

[7] V. V. Jikov, S. M. Kozlov, and O. A. Oleĭnik. *Homogenization of differential operators and integral functionals*. Springer-Verlag, Berlin, 1994. Translated from the Russian by G. A. Yosifian [G. A. Iosif′yan].

[8] J. Keener and A. Panfilov. A biophysical model for defibrillation of cardiac tissuev. *Biophys.*, 71(3):1335–1345, 1996.

[9] J. P. Keener. The effect of gap junctional distribution on defibrillation. *Chaos: An Interdisciplinary Journal of Nonlinear Science*, 8(1):175–187, 1998.

[10] F. Murat and L. Tartar. *H*-convergence. In *Topics in the mathematical modelling of composite materials*, volume 31 of *Progr. Nonlinear Differential Equations Appl.*, pages 21–43. Birkhäuser Boston, Boston, MA, 1997.

[11] J. C. Neu and W. Krassowska. Homogenization of syncytial tissues. *Crit. Rev. Biomed. Eng.*, 21(2):137–199, 1993.

[12] M. Pennacchio, G. Savaré, and P. Colli Franzone. Multiscale modeling for the bioelectric activity of the heart. *SIAM J. Math. Anal.*, 37(4):1333–1370 (electronic), 2005.

[13] S. Spagnolo. Sulla convergenza di soluzioni di equazioni paraboliche ed ellittiche. *Ann. Scuola Norm. Sup. Pisa (3) 22 (1968), 571-597; errata, ibid. (3)*, 22:673, 1968.

[14] S. Spagnolo. Convergence in energy for elliptic operators. In *Numerical solution of partial differential equations, III (Proc. Third Sympos. (SYNSPADE), Univ. Maryland, College Park, Md., 1975)*, pages 469–498. Academic Press, New York, 1976.

[15] L. Tartar. Problèmes de contrôle des coefficients dans des équations aux dérivées partielles. In *Control theory, numerical methods and computer systems modelling (Internat. Sympos., IRIA LABORIA, Rocquencourt, 1974)*, pages 420–426. Lecture Notes in Econom. and Math. Systems, Vol. 107. Springer, Berlin, 1975.